Orbital and Structural Evolution of Triton

Rishi Sugla

Advisors: Saswata Hier-Majumder
Douglas Hamilton
Vedran Lekić

GEOL393H
26 April 2013

Abstract

Triton, Neptune's largest moon, is one of the coldest bodies in our universe with a surface temperature of 38 K. Even at this low temperature, Triton may have sustained an ammonia-rich subsurface ocean throughout its history. The potential presence of this ocean relies on Triton's orbital evolution and internal composition through time. The orbital evolution refers to changes in the semi-major axis, eccentricity, and orbital frequency of Triton over time. The changes in internal composition, or structural evolution, refer to the progressive crystallization of Tritons ammonia rich subsurface ocean. After its capture by Neptune from a heliocentric binary, Triton's orbit was rapidly circularized. The circularization of Triton's orbit around Neptune most likely occurred during the first few hundred Ma after the formation of our solar system. Subsequently, the orbital frequency and semi-major axis of Triton's orbit evolved to its current value. During the first semester of my thesis, I investigate the evolution of orbital frequency and semi-major axis of Triton using the governing ordinary differential equations from orbital dynamics.

Due to the retrograde nature of Triton's orbit, its semi-major axis decays over time. Results from my simulation indicate that Triton's semi-major axis decays slowly, by approximately 6% over 3.5 Ga past the circularization of its orbit. This leads to an approximately 8% increase in orbital frequency over this period. The normalized tidal dissipation, however, increases by nearly 60% within this time period. The increase in average tidal dissipation helps warming the ice shell and will likely retard the rate of freezing of the subsurface ocean. This thesis hypothesizes that Triton's spin-up increases tidal heating enough to sustain a polar subsurface ocean. As spin-up occurs, the magnitude of tidal dissipation within the ice shell increases. Tidal dissipation predominantly acts of the base of the ice shell near the polar regions. As progressive increases in tidal dissipation due to Triton's spin-up occur, crystallization rates of the ice shell decrease. At values as low as 8×10^{-5}, models show maintains a 200km thick ocean beneath its icy outer shell. As eccentricities decrease further, polar oceans rather than global oceans become increasingly likely. My calculations show that in most cases a global subsurface ocean is not sustained over time. In many cases, however, a polar subsurface ocean is sustained until present day for a wide range of variable parameters. Therefore, I accept the hypothesis that Triton's spin-increases tidal heating enough to sustain a polar susburface ocean.

Contents

List of Figures

1 Introduction

Triton is the largest of Neptune's thirteen moons with a radius of 1325 km and a mass of 2.14×10^{22} kg. Over half of Triton's surface is composed of N_2 in solid solution with carbon monoxide (CO) and methane (CH_4). The other half of Triton's surface is composed of carbon dioxide (CO_2) and water ice (H_2O) (*McKinnon and Kirk*, 2007). Despite the abundance of volatiles on its surface, data from the *Voyager* mission suggests that Triton's density is 2065 kg m^{-3}, high enough to require a core composed of both silicate and metal. The interior of Triton is likely composed of a metallic core at its center. Above the metallic core, a silicate mantle containing radioactive elements is likely present. The schematic diagram in Figure 1 outlines a likely interior structure of Triton (*Gaeman et al.*, 2012).The heating from these radioactive elements could contribute to the potential subsurface ocean within Triton.

Current orbital parameters provide us with some clue regarding Triton's origin. The orbit of Triton is retrograde and has high inclination of 156.85 degrees. By comparison, Earth's moon has an inclination of 1.54 degrees. Such a retrograde orbit and high inclination indicate that Triton was captured by Neptune after originally being in a heliocentric orbit around the sun (*Agnor and Hamilton*, 2006). Triton's similar density to Kuiper Belt objects indicate that it was formed in that area (*McKinnon and Kirk*, 2007).

The following subsections discuss the observed geologic features on Triton's surface and the orbital history of Triton.

1.1 Geology and current internal structure of Triton

Triton contains several recent geologic features. These features include an area of quasi-linear ridges and dimples formed by diapirism, a poorly understood polar region, and undulating high plains (*McKinnon and Kirk*, 2007). The undulating high plains form from icy volcanism. The icy volcanism manifests as a series of vents and terrestrial volcanic calderas. The current composition of the icy lavas is currently unknown. The region of quasi-linear ridges and dimples on Triton are commonly referred to as cantaloupe terrain. This region displays a well ordered structural pattern of kidney shaped depressions known as cavi. The uniform size of the cavi indicate their diapric origin. The region of cantaloupe terrain also contains well formed parallel ridges which bound a central trough (*McKinnon and Kirk*, 2007). These ridges are 6-10 km across crest-to-crest and several hundred meters high. Fissures in this region are less numerous and are 2-3 km wide. Images from *Voyager* show that some areas of the cantaloupe terrain are engulfed by up to a few hundred meters of bright ice. The overall thickness of the polar ice is believed to be less than 1 km thick. Although this region is a polar cap, the icy terrain may behave as if it is glaciated due to warming from deposits of volatile ice such as N_2 (*McKinnon and Kirk*, 2007).

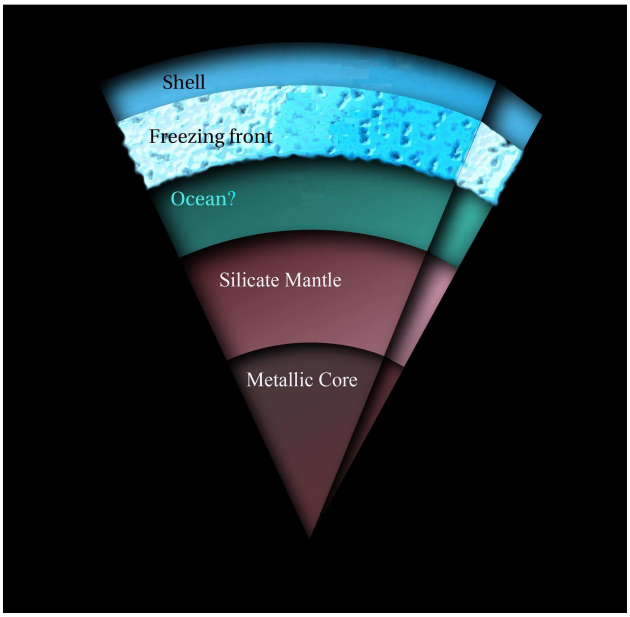

Figure 1: Cross sectional view of Triton's interior (not to scale), based on *Gaeman et al.* (2012).

Triton is likely geologically active. *Stern and Mckinnon* (2000) suggest that the surface age of Triton is less than 100 Ma based on crater counts. The young surface age, combined with the observed structures on Triton's surface indicate that these features were created within the last 100 Ma. The driving force behind the geologic activity, however, is still debated.

One explanation suggests that Triton's current geologic activity is due to deformation due to tidal diurnal stress within Triton as it orbits Neptune (*Prockter et al.*, 2005). A study by *McKinnon and Kirk* (2007), however, suggests that tidal diurnal stress alone would be an insufficient mechanism to generate the previously mentioned geologic features. Triton's low eccentricity does not result in a strong enough tidal forcing to create tide-based geologic features such as those seen on Europa (*Greenberg et al.*, 1998).

Gaeman et al. (2012) used the abundances of these radiogenic elements to model heat transport within the interior of Triton over time. This model dynamically incorporated thickening and thinning of Triton's ice shell while examining the coupling between the ice shell-ocean in Triton. The model of ice sheet growth or retreat was examined as a function of different eccentricities. *Gaeman et al.* (2012) found that even at low values of Triton's eccentricity, a subsurface ocean may have been sustained within its interior over a geologically

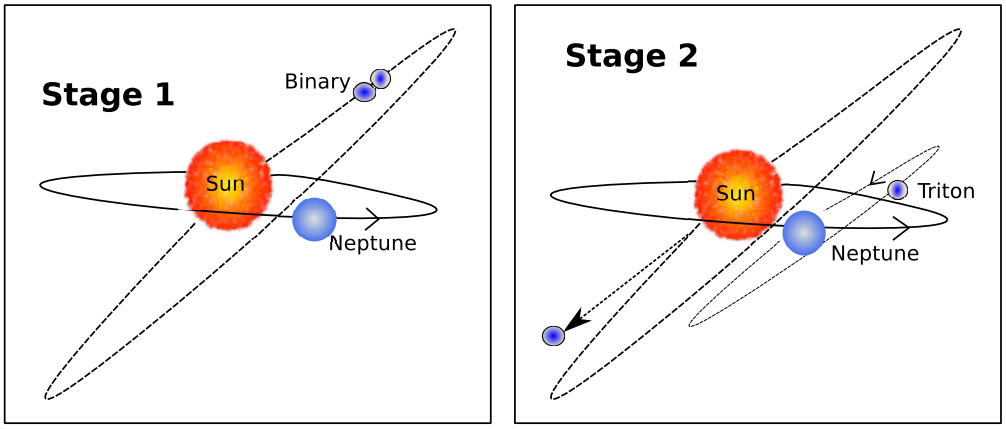

Figure 2: A schematic diagram outlining Triton's capture by Neptune. During stage 1, Triton, one of the objects in the binary, orbits around the Sun. During stage 2, Triton is captured by Neptune's gravity.

significant period of time.

The changes in orbital evolution, however, are poorly constrained. This work seeks to further constrain orbital evolution, namely semi-major axis and eccentricity, so it may be coupled with previous models of structural evolution developed by *Gaeman et al.* (2012). If a subsurface ocean exists within Triton, it may have the potential to sustain life within its ammonia-rich subsurface ocean. In addition, it is possible that its silicate mantle may potentially contain silicate-based life, however this is less likely (*McKinnon and Kirk*, 2007).

1.2 Orbital History

There are two proposed methods for the capture of Triton into Neptune's orbit. The first hypothesis suggests that Triton was in a binary system in a heliocentric orbit as shown in Figure 2. As the binary system approached Triton, its orbit interacted with the gravitational field of Neptune resulting in capture (*Agnor and Hamilton*, 2006). The second mechanism for capture is a satellite coming into repeated contact with Neptune by hydrodynamic drag, which would result in net energy dissipation from the system (*McKinnon and Leith*, 1995). The latter is unlikely because of the high number of passes which would have had to occur in order for the capture to be likely (*Agnor and Hamilton*, 2006).

Once capture occurs, the orbit of the satellite would circularize to its current, nearly circular eccentricity. The energy loss from these systems would come from tidal dissipation of energy in Triton caused by Neptune as the satellite continued its orbit (*Ross and Schubert*,

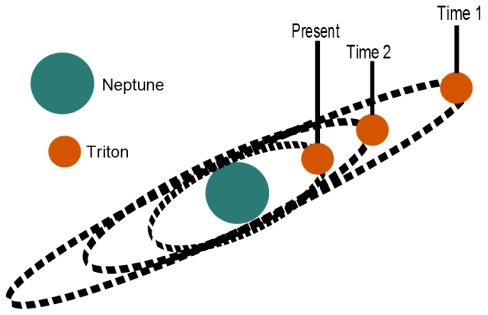

Figure 3: Diagram of circularization of Triton (not to scale).

1990). An alternative hypothesis suggests that this capture caused a perturbation of pre-existing satellites orbiting Neptune. The perturbed satellites then collided to form a debris disk around Neptune. The interaction of Triton with this debris disk increased the rate of energy loss of the satellite, leading to an increased rate of circularization (*Ćuk and Gladman*, 2005). Both hypotheses for capture suggest that the circularization of Triton occurred in a short time interval (10^5 years).

The rapid circularization of Triton contributed a large amount of energy into this system (Figure 3) (*Ross and Schubert*, 1990). *Ross and Schubert* (1990) hypothesize that this energy would have inevitably created a subsurface ocean within Triton. A mechanism sustaining this subsurface ocean post-circularization is tidal blanketing (*Gaeman et al.*, 2012). Tidal dissipation, while only a modest source of heat compared to the radiogenic elements within Triton, plays an important role in sustaining the post-circularized subsurface ocean. This is because tidal dissipation does not act evenly on the ice shell, instead acting predominantly on the basal surface of the ice shell. This mechanism reduces the basal heat flux on the ice shell and slows the crystallization of the ice shell overlying the subsurface ocean (*Gaeman et al.*, 2012).

While the model constructed by *Gaeman et al.* (2012) uses varying values of eccentricity in order to examine its effect on the structural evolution of Triton, it does not take into account the dynamic values of semi-major axis it changed over time. Since tidal blanketing, caused by tidal dissipation of heating, plays a major role in ice sheet growth or retreat the orbital evolution of Triton must be further constrained. A model of orbital evolution is constructed in this study to determine how it changed over time. Eventually, this model will be coupled with the model of structural evolution developed by *Gaeman et al.* (2012)

to better understand the potential of a subsurface ocean within Triton.

2 Methods

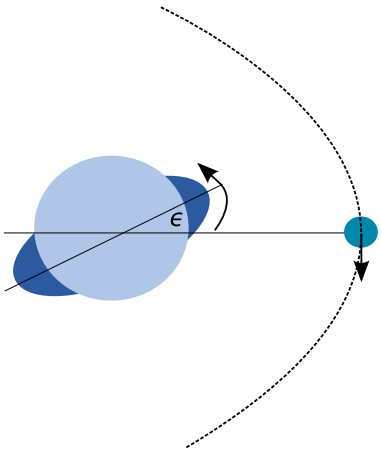

Figure 4: A schematic diagram depicting the tide raised in a two body system. The quantity ϵ depicts the lag between the tidal bulge and the perturbing body.

The coupled orbital and structural evolution models for this thesis must take into account three main parameters which directly relate to ice shell growth and retreat throughout time. For Triton, the thermal, orbital, and structural evolution must all be considered. These three factors directly feed into one another. The structure and semi major axis of Triton at an intitial time will alter the tidal dissipation in Triton's subsurface ocean which existed post-capture. The tidal dissipation of energy will then directly affect the conductive heat transder of laten heat of crystallization through the base of the ice shell. This tidal dissipation is calculated by a previously constructed numerical code known as TiRADE. The change in conduction corresponds a dynamic freezing rate which well change as a result. Finally, the freezing rate will change the structure of the ice shell and the loop will begin again. This process is governed by three differential equations which describe the thermal, orbital, and structural evolution. These governing equations will be described in further detail below. A model of this process can be seen in Figure 5.

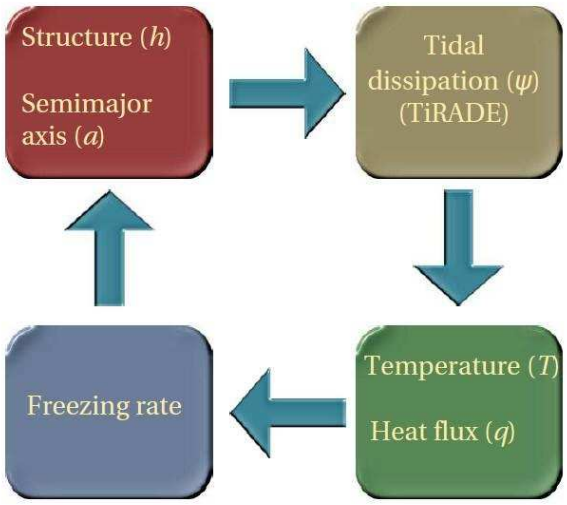

Figure 5: Model of the numerical calculations in the orbital-structural-thermal evolution model.

2.1 Orbital evolution

In this thesis, the Neptune-Triton system is treated as a two body system and neglect the gravitational effects of Neptune's other moons. In the simple two-body system, illustrated in the schematic Figure 4, the perturbing body (Neptune) raises a tide in the perturbed body (Triton). If the orbital frequencies of the two bodies are different, the tidal bulge, indicated by the dark shaded regions either precede or lag the perturbing body. As the total energy and the angular momentum in the system must be conserved, the energy required to raise the tide is dissipated through changes in the orbit (*Murray and Dermott*, 1999, Ch 4.9). The angle of lag ϵ depicted in Figure 4 is related to the dissipation factor Q by the relation,

$$\sin 2\epsilon = -\frac{1}{Q}. \tag{1}$$

In the Neptune-Triton system, Triton exerts a torque and tidal bulge onto Neptune throughout its orbit *Murray and Dermott* (1999). This torque is related to the orbital angular velocity of Triton in its orbit. Because energy within the system must be conserved, the sum of the energy in the system is equal to the rotational energy of the planet and the orbital energy of the system. Thus, the change of energy within the system may be described by two Ordinary Differential Equations which are the governing equations for the orbital evolution model.

The eccentricity dampening rate is an important component of this model. The eccentricity dampening rate can be described by,

$$\frac{\mathrm{d}e}{\mathrm{d}t} = -e\frac{63}{4}\frac{M_n}{M_N}\left(\frac{R_T}{a}\right)^5 \frac{u_T Q_T}{n}, \tag{2}$$

Where t is the time since orbit circularization, e is the eccentricity, and M_T and M_N are masses of Triton and Neptune, respectively. Q_N is the tidal dissipation factor of Neptune and n is the orbital frequency of Triton. Q_N is a dimensionless parameters that measures the loss-rate of energy from tides, known as the quality factor (*Goldreich and Soter*, 1966). The semimajor axis of Triton also changes with time, assuming a small orbital eccentricity, and can be described by,

$$\frac{\mathrm{d}a}{\mathrm{d}t} = -\frac{3k_2}{Q_N}\frac{M_T}{M_N}\left(\frac{R_N}{a}\right)^5 an, \tag{3}$$

Where t is time since orbit circularization, k_2 is the tidal Love number of Triton, and R_N is the radius of Neptune. The k_2 tidal Love number is a dimensionless parameter which describes the deformation of a rigid body due to tidal forces. The values of these variables may be found in Table 1 below. Based on Kepler's third law, we can relate the orbital frequency n to the semi-major axis by the relation,

$$n = \sqrt{\frac{GM_N}{4\pi^2 a^3}}, \tag{4}$$

where G is the gravitational constant.

The mechanical energy required to raise the tide is dissipated by variation in the semi-major axis and orbital frequency. This variation, however, feeds back into the average rate of tidal dissipation, $\dot{E}$, through orbital frequency and orbital eccentricity e following

$$\dot{E} \propto e^2 a^5. \tag{5}$$

Following the orbital evolution of Triton, if Triton's orbital eccentricity is damped to a near constant value shortly after it's capture, then I can express the normalized tidal dissipation as a function of time in the following manner,

$$\frac{\dot{E}(t)}{\dot{E}(0)} = \left(\frac{a(t)}{a(0)}\right)^5, \tag{6}$$

where $\dot{E}(0)$ is the tidal dissipation immediately after circularization, and $a(0)$ is the semi-major axis immediately after circularization. Solving equation 3, I can track the evolution of the tidal dissipation resulting from Triton's orbital evolution.

In this thesis, I solved the ODE in equation 3 numerically using the Fourth Order Runge-Kutta Method (RK4). I provide an initial condition for the semi-major axis corresponding to the apoapsis at a reference eccentricity e_0, as

$$a(0) = 14C_N(1 + e_0). \tag{7}$$

The current value of Triton's semi-major axis is approximately 14 times Neptune's radius ($14C_N$) (*Ćuk and Gladman*, 2005), and the initial orbital eccentricity $e_0 = 0.05$. The value of Q_N in the governing equations has only recently began to be constrained and may have a range of potential values (*Zhang and Hamilton*, 2008; *Goldreich and Soter*, 1966). The different values of Q will be tested and the correct value for the system be supplied into the code.

In the following section, I present the method for analyzing errors arising from the numerical solution.

Symbol	Description	Units	Reference
C_N	Radius of Neptune	27764 km	*McKinnon and Kirk* (2007)
a	Semimajor axis of Triton	354760 x 10^3	*McKinnon and Leith* (1995)
K_{2T}	Love number; Triton	0.41	*Zhang and Hamilton* (2008)
Q_N	Quality factor; Neptune	12000	*Zhang and Hamilton* (2008)
M_T	Mass of Triton	2.140 x 10^{22} kg	*McKinnon and Kirk* (2007)
M_N	Mass of Neptune	1.0241 x 10^{26} kg	*McKinnon and Kirk* (2007)
α	Moment of inertia factor	$\frac{2}{5}$	

Table 1: Table of constants used in the calculation

2.2 Thermal and structural evolution

Structural and thermal evoltuion are primarily controlled by heat conduction within the ice shell and latent heat of crystillazation. The first PDE I examine is,

$$\frac{\partial T}{\partial t} = -\frac{k}{pc_p}\nabla^2 T + \psi \tag{8}$$

Where T is the temperature within the ice shell, k is the thermal conductivity, p is the density, c_p is the heat capacity, and ψ is the tidal dissipation within the ice shell. This equation represents the conservation of energy within the ice shell, and therefore the ice shell's capacity to propogate or retreat. As crystallization continues to occur boundary layer between the ice shell and ocean continues to move.

This equation does not take into account the movement of the ice-shell ocean boundary as the subsurface ocean crystallizes, however. A seperate equation must be used to take into account the movement of the ice-shell ocean boundary.

$$p\triangle H\frac{\mathrm{d}h(t)}{\mathrm{d}t} = k\nabla T\cdot\hat{r} \mid h(t) - Q_r(t) \mid h(t) \tag{9}$$

where the term on the right hand side represents the radial basal heat flux and the second term on the right hand side represents heat flux arusing from the decay of radiocative elements in Triton's silicate mantle.

The differential equations were modelled by using the Finite Element Model Dynamics of Melt Migration and Storage (DyMMS). This finite element model creates a two-dimensional grid of quadratic quadrilateral elements across Triton's interior. A quadratic quadrilateral element is characterized by a quadratic shape function in two dimensions. These elements have eight nodes which are numerical solved for using DyMMS. The numerical solutions calculate the numerical values at the center of each quadratic quadrilateral element. The temperature, heat flux, and ice-sheet ocean layer were interpolated at each individual time step from the governing equations. Based on the results of this interpolation, I can repeat the calculations and continue to advance the ice sheet for different time steps. A sample grid composed of quadratic quadrilaterals can be found in Figure 6.

2.3 Error analysis

Source of error comes from discretizing the governing ODE. Discretization refers to approximating a continuous function into discrete counterparts. I can estimate this error by using the MATLAB code to obtain a numerical solution $f(\bar{x})$ to a problem, whose exact solution $f(x)$ is known at each point of the domain x. Then I define the error ε associated with the numerical solution at each point in the domain as

$$\varepsilon = f(x) - \bar{f}(x), \tag{10}$$

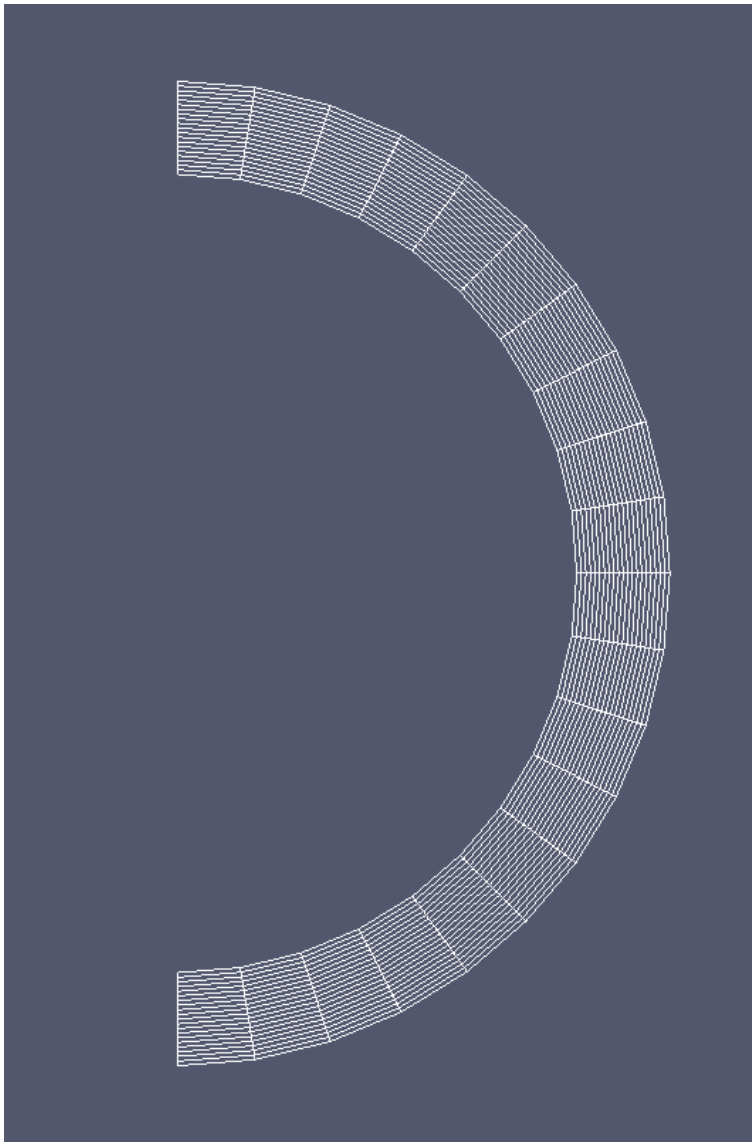

Figure 6: Mesh grid composed of quadratic quadrilaterals. Propogation of ice sheet advancement was solved using Finite Element Method calculation in DyMMS.

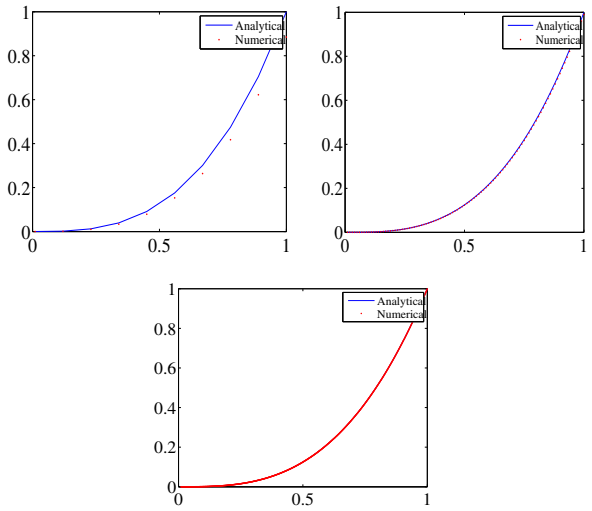

Figure 7: Numerical and analytical solutions for the function $f(x) = x^3$ for varying step sizes. The top left graph has 10 steps, the top right 100, and the bottom center 1000.

Since the numerical solution is obtained over an array of points, it is useful to define the L_1, L_2, and L_∞ norms associated with the error. These norms are defined as,

$$L_1 = \sum_{k=1}^{N} \left| f(x_k) - \bar{f}(x_k) \right|, \tag{11}$$

$$L_2 = \sum_{k=1}^{N} \sqrt{\left| f(x_k) - \bar{f}(x_k) \right|^2}, \tag{12}$$

and

$$L_\infty = \max \left| f(x_k) - \bar{f}(x_k) \right|, \tag{13}$$

where N is the size of the grid. As the grid size increases, the error arising from discretization decreases. The decrease in the error will be depicted by decrease in the associated norms with an increase in the grid size. I can define the following criterion for minimizing the error associated with grid size,

$$\frac{\partial L_x}{\partial N} \to 0, \tag{14}$$

where L_x represents one of the norms defined above.

To test the errors associated with grid size, I carried out a series of benchmark integrals, where the numerically computed value of the integral was compared with the known exact

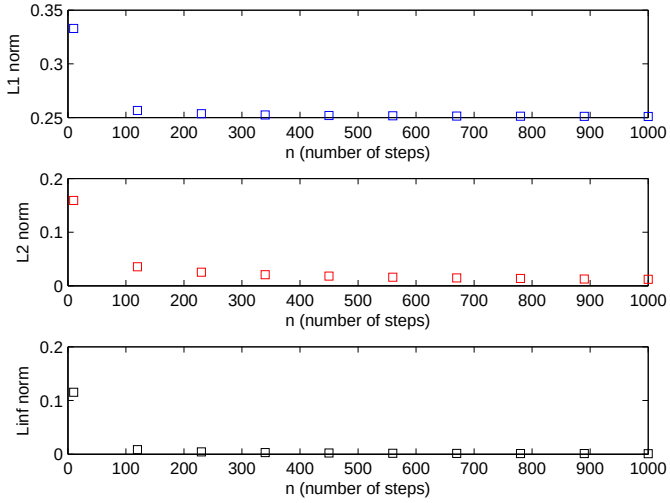

Figure 8: A plot of L_1, L_2, and L_∞ norms as a function of grid size for the exact solution $f(x) = x^3$.

solution. One specific case is demonstrated in the series of plots in Figure 7. In these plots, I compared the numerical value of the integral $\int_0^x 3x^2 \mathrm{d}x$ with the exact value x^3 over the range [0,1], for a number of different grid sizes.

The series of plots in Figure 8 display the L_1, L_2, and L_∞ norms as a function of the grid size for these tests. As the plots indicate, the slopes for all norms become nearly flat for grid sizes above 400. In the simulations, I use a grid size of 1000, well above the the threshold where the criterion outlined in equation 14 is reached.

An additional source of error is the tidal love number k_2 and the quality factor, Q_N. In my model, I use a single value for $\frac{k_2}{Q_N}$ in Equation 3. This, however, is unrealistic because k_2 is a nondimensional measure of the rigidity of a planetary body when exposed to tidal forces. As Triton's ice-shell boundary propogates, the value of k_2 will change with time as well. To determine the effect that changes in $\frac{k_2}{Q_N}$ have on eccentricity dampening and semimajor axis, I constructed a model varying $\frac{k_2}{Q_N}$ by an order of magnitude. The model was executed for orders of magnitude ranging for 10^{-2} to 10^{-4}. The results of this model will be shown in the next section.

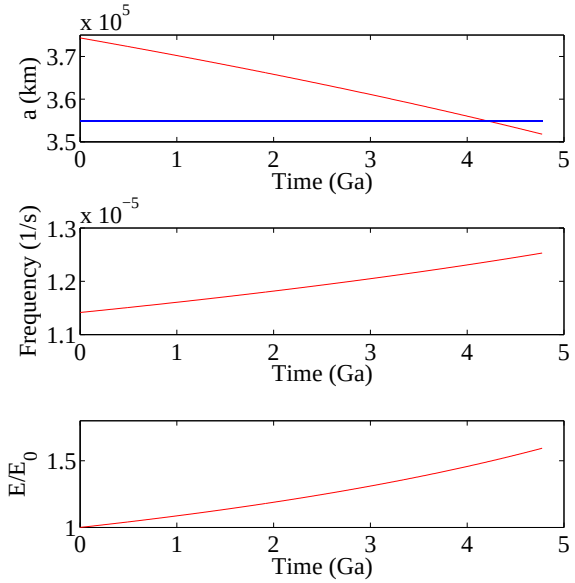

Figure 9: A schematic diagram outlining Triton's capture by Neptune. During stage 1, Triton, one of the objects in the binary, orbits around the Sun. During stage 2, Triton is captured by Neptune's gravity.

3 Results

Triton's unique retrograde orbit leads it to slowly spiral in towards Neptune. As the plot in the top panel of Figure 9 indicates, over 3.5 Ga, Triton's semi-major axis decays by approximately 6%. The slow decay of the orbit leads to an increase in the orbital frequency, following Kepler's third law. The plot in the middle panel of Figure 9 depict that the orbital frequency of Triton increasesr gently, by approximately 8% over this time period.

Despite the relatively modest changes in the semi-major axis and orbital frequency, the average tidal dissipation in Triton's interior changes more substantially. As the plot in the lowermost panel in Figure 9 indicates, the normalized tidal heating $\dot{E}(t)/\dot{E}(0)$, defined in equation 6, increases by nearly 50% over the course of time. The large increase in tidal dissipation has a number of important consequences for the structural evolution of Triton. All other parameters remaining constant, an increase in the available tidal heating, which partitions into Triton's icy crust, warms up the crust and slows down the rate of freezing. As a result, this slow spin-up of Triton's orbit likely enhances the chances of survival of a subsurface ocean.

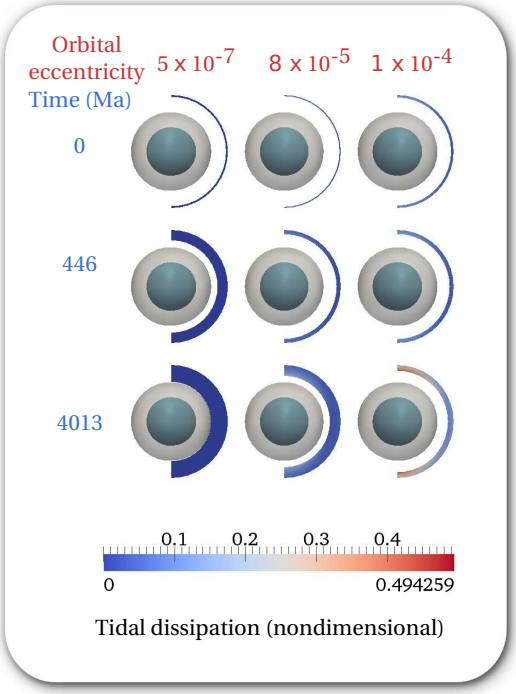

Figure 10: Variation of tidal dissipation within Triton over time.

This orbital evolution model was then coupled with the structural and thermal evolution models as described by Figure 5. The result of these coupled models are shown in Figures 10, 11, and 12 below. In Figure 10 we notice that at low eccentricities, tidal disspiation falls to zero in 4 Ga. Tidal dissipation continues to be a factor, however, in eccentricties of $8x10^{-5}$ or higher. At even higher eccentricities, we notice that tidal dissipation remains quite strong over time.

Both radial flux and and variation of temperature over time vary similarly to tidal dissipation. As by Figures 11 and 12, a subsurface ocean may be sustained at suffieciently low eccentricities. The ice shell-ocean front fails to completely reach the core in all but the lowest eccentricities in both these scenarios.

As previously mentioned in the error section, values of k_2 and Q_N directly affect the orbital evolution (and therefore the structural evolution) of Triton. The outputs of my

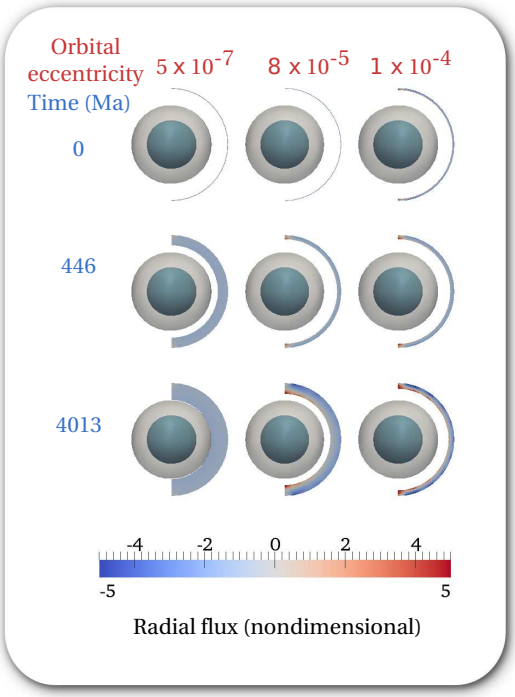

Figure 11: Variation of radial flux within Triton over time.

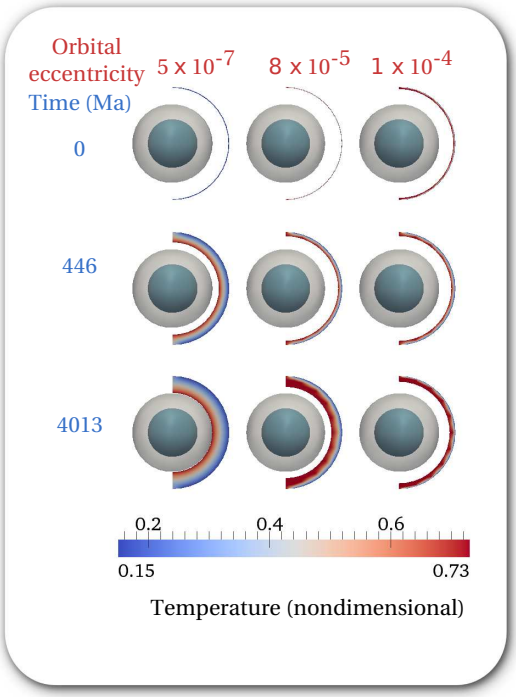

Figure 12: Variation of temperature within Triton over time.

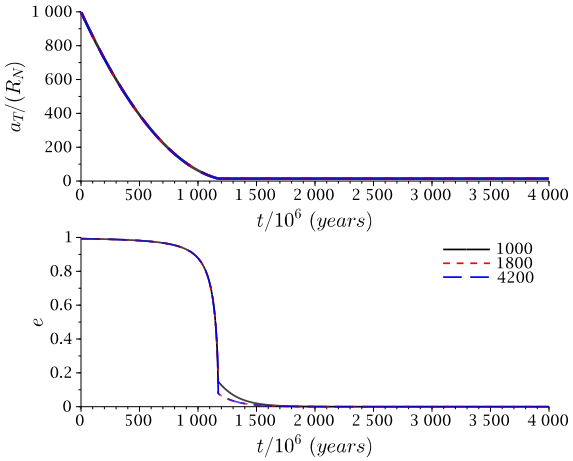

Figure 13: The ratio of Triton's semi-major axis and Neptune's radius with respect to time (top) and eccentricity dampening rate (bottom)for a for a $\frac{k_2}{Q_N}$ with an order of magnitude of 10^{-4}.

model can be seen in Figures 13, 14, and 15. The different colored lines in these figures represent different gridsizes which allow me to exam the error based on gridsize. The dark blue lines are associated with the highest gridsize and therefore the least amount of error. Figure 13 shows the slowest rate of change of semimajor axis and eccentricity dampening rate and corresponds to the lowest value of $\frac{k_2}{Q_N}$ at a magnitude of 10^{-4}. In this scenario, semi-major axis of Triton reaches its current state in A low value of $\frac{k_2}{Q_N}$ indicates that Triton is more rigid. As this value increases in size, the eccentricity dampening rate and rate of decrease in semimajor axis increases (Figures 14 and 15).

4 Suggestion for Future Work

At the end of the previous section I examined the affect that a change in $\frac{k_2}{Q_N}$ may have on the orbital evolution (and therefore structure) of Triton. For the coupled structural and orbital evolution models, however, a single value for this parameter was used. Future models should be able to incorporate dynamic values of $\frac{k_2}{Q_N}$ as it changes with internal structure. Incorporating this into the coupled structural and orbital evolution model will allow us to understand the potential likelihood of a subsurface ocean. Furthermore, the current $\frac{k_2}{Q_N}$ value of Triton needs to be better constrained. The magnitudes used in our error analysis are predminantly based on numerical models. If the current $\frac{k_2}{Q_N}$ value today can be

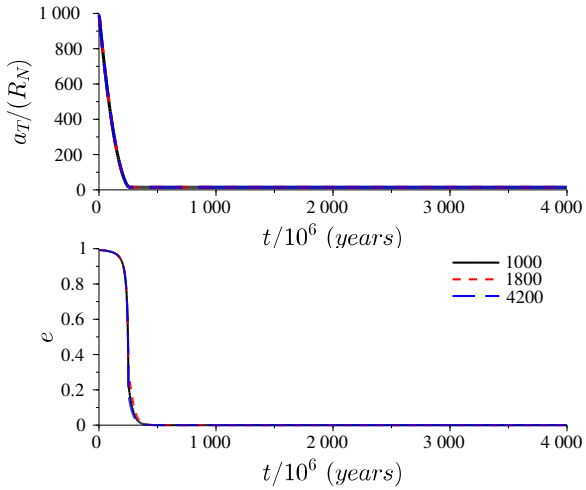

Figure 14: The ratio of Triton's semi-major axis and Neptune's radius with respect to time (top) and eccentricity dampening rate (bottom)for a for a $\frac{k_2}{Q_N}$ with an order of magnitude of 10^{-3}.

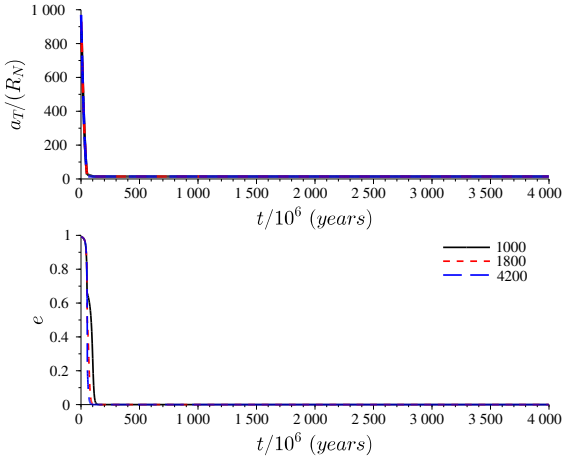

Figure 15: The ratio of Triton's semi-major axis and Neptune's radius with respect to time (top) and eccentricity dampening rate (bottom)for a for a $\frac{k_2}{Q_N}$ with an order of magnitude of 10^{-2}.

experimentally constrained, it should allow us to better determine the initial value of $\frac{k_2}{Q_N}$ to use at time of capture.

5 Discussion

In a previous work, *Gaeman et al.* (2012) demonstrated that tidal heating arising from even low constant eccentricities can warm up the base of Triton's icy shell and slow down the rate of freezing. In this analysis, however, both eccentricity and orbital frequency remained constant. As the result from this work indicates, the increase in Triton's orbital frequency and the corresponding increase in tidal dissipation is nontrivial over geologic time. Such an increase in tidal dissipation only occurs due to Triton's unique retrograde orbit. For example, in the Earth-Moon system, the Moon recedes from the Earth while the length of the day gradually increases on Earth.

In the coupled orbital-structural-thermal evolution model we notice that a the subsurface ocean fails to crystallize for all but the lowest eccentricities. The effects of tidal blanketing, most prominently visible in Figure 12, show the basal layer of the propogating ice shell at a higher temperature than the upper portions. This increased basal heating seems to sustain the subsurface ocean through time. At lower eccentricities, the subsurface ocean completely crystallizes over time. The presence of a subsurface ocean based on these calculates is certainly plausible. Specifically, polar oceans become increasingly likely at lower initial eccentricities of Triton post-capture. The effect of tidal blanketing at most eccentricities slows down the rate of crystallization drastically. This effect is most prominent in the polar regions.

Based on my current calculations, I conclude that a polar subsurface ocean may exist on Triton today. While a global subsurface ocean is also possible, it remains far less likely that it is currently present under the outer ice-shell.

References

Agnor, C. B., and D. P. Hamilton, Neptune's capture of its moon triton in a binary-planet gravitational encounter, *Nature*, *441*, 192–94, 2006.

Ćuk, M., and B. J. Gladman, Constraints on the orbital evolution of triton, *ASTROPHYSICAL JOURNAL*, *626*, L113–L116, 2005.

Gaeman, J. S., S. Hier-Majumder, and J. a. Roberts, Sustainability of a subsurface ocean within triton's interior, *Icarus*, *220*, 339–447, 2012.

Goldreich, P., and S. Soter, Q in the solar system, *Icarus*, *5*, 375 – 389, 1966.

Greenberg, R., P. Geissler, G. Hoppa, B. Tufts, D. D. Durda, R. Pappalardo, J. W. Head, R. Greeley, R. Sullivan, and M. H. Carr, Tectonic processes on europa: Tidal stresses, mechanical response, and visible features, *Icarus*, *135*, 64 – 78, 1998.

McKinnon, W. B., and R. L. Kirk, *Encyclopedia of the Solar System*, chap. Triton, pp. 483–502, Academic Press, 2007.

McKinnon, W. B., and A. C. Leith, Gas drag and the orbital evolution of a captured triton, *Icarus*, *118*, 392–413, 1995.

Murray, C. D., and S. F. Dermott, *Solar System Dynamics*, Cambridge University Press, 1999.

Prockter, L. M., F. Nimmo, and R. Pappalardo, A shear heating origin for ridges on triton, *Geophysical Research Letters*, *32*, 2005.

Ross, M. N., and G. Schubert, The coupled orbital and thermal evolution of triton, *Geophysical Research Letter*, *17*, 1749–752, 1990.

Stern, S. A., and W. B. Mckinnon, FLUXES : EVIDENCE FOR SMALL KUIPER BELT OBJECTS AND RECENT GEOLOGICAL ACTIVITY, *The Astronomical Journal*, *119*, 945–952, 2000.

Zhang, K., and D. P. Hamilton, Orbital resonances in the inner neptunian system:ii. resonant history of proteus, larissa, galatea, and despina, *Icarus*, *193*, 267 – 282, 2008.